Pergamon

Atmospheric Environment Vol. 30, No. 23, pp. 3995–4006, 1996

1352–2310/96 $15.00 + 0.00

PII: S1352–2310(96)00123–9

AIR EXCHANGE WITHIN THE BUDDHIST CAVE TEMPLES AT YUNGANG, CHINA

CHRISTOS S. CHRISTOFOROU, LYNN G. SALMON and GLEN R. CASS*

Mechanical Engineering Department and Environmental Quality Laboratory, MC 138-78, California Institute of Technology, Pasadena, CA 91125, U.S.A.

(*First received* 28 *August* 1995 *and in final form* 20 *March* 1996)

Abstract—The Buddhist cave temples at Yungang, China, are subjected to rapid soiling due to the deposition of airborne particles onto the thousands of statues in those caves. During April 1991, temperatures and air exchange rates were measured at Caves 6 and 9 at Yungang in order to establish baseline parameters necessary for modeling the air flow that carries air pollutant particles into and out of the caves. Air flow through the caves was found to be governed by a natural convection flow pattern that is driven by the difference between the temperature of the outdoor air and the temperature of the interior walls of the caves. During the day, warm outdoor air enters the upper entrances to the caves, is cooled by the cave walls and flows out through the ground level exits from the caves, while during the night the situation is reversed. The average air velocity at the entrance of Cave 9 during the course of the experiment was 0.274 $m\,s^{-1}$, amounting to an air exchange rate of 121 $m^3\,min^{-1}$, which achieves one complete air change within Cave 9 in only 4.3 min on average. Cave 6 is larger than Cave 9, and air flow through Cave 6 is restricted by the presence of the wooden temple structure that is built over the entrances to Cave 6, yielding times to achieve a complete air exchange within Cave 6 that are typically 4 times longer than at Cave 9 under the April conditions studied. A theoretical model has been developed that takes as input cave wall and outdoor air temperatures and then predicts indoor air temperatures as well as air velocities at the entrance to the caves. The model can be used to predict air flows through the caves in the presence of increased resistance to air flow such as may occur following the future installation of filtration systems for particle removal at the caves. Copyright © 1996 Elsevier Science Ltd

Key word index: Yungang Grottoes, cave temples, fluid mechanics, natural convection, mathematical modeling.

INTRODUCTION

During April 1991, an environmental monitoring experiment was conducted at the Buddhist cave temples at Yungang in the northern part of Shanxi Province in the People's Republic of China. The purpose was to characterize the exposure of the grottoes to air pollutants in a manner that will establish a basis for the future protection of the grottoes from air pollution damage. The present paper describes the processes that drive air flow through these caves. That air flow acts to transport air pollutant particles into the caves from the outdoors. An understanding of the air flow patterns at the Yungang Grottoes is critical to an understanding of the air pollution problems that affect these cave temples.

The Yungang ("Cloud Hill") Grottoes are a collection of man-made caves excavated into the side of a steep sandstone cliff. Construction of the caves began in the 5th century AD under the supervision of the Northern Wei emperors. There are 53 Buddhist caves, 21 larger ones and 32 smaller caves and niches. The larger caves are similar in architecture. A passage way dug into the cliff face at ground level opens into a large man-made cavern excavated behind the cliff face. These rooms within the cliff are typically rectangular, between 10 and 15 m long on each side and approximately 12.5 m high. At the rear of some caverns, and at the center of others there is a huge pillar that stretches from the cave floor nearly to the ceiling. This central column typically is carved into a monumental statue of the Buddha, but there are examples of pillars that take the form of a pagoda. The interior walls of these chambers are decorated with more than 51,000 bas-reliefs and statues ranging from several centimeters in height to more than 10 m in height, that depict Buddhist deities and scenes from the life of the Buddha. Some of these stone carvings still retain their historical coloring (Cox, 1957; Sickman and Soper, 1968; Knauer, 1983).

The larger caves usually have an entry at ground level and another opening through the cliff face to the outdoors at about the third-floor level. During antiquity these entrances to the larger caves were sheltered by wooden temple structures one room deep

*To whom correspondence should be addressed.

and several stories high that were built against the outside front of the cliff face. Repairs to the cave temples were made during the Liao and Ching Dynasties, but by the early 1900s visitors report that the caves had fallen into a state of neglect (Cox, 1957). At present, only Caves 5 and 6 still retain the wooden temple structures in front of their entrances. Today agencies of the Chinese government are actively trying to protect the grottoes: the Yungang Grottoes Institute has been established to care for the caves; the area immediately adjacent to the grottoes has been turned into a park and the caves are open to visits by the public.

The Yungang Grottoes are situated about 16 km west of the industrial city of Datong, in the middle of one of China's largest coal mining regions. As a result, the Grottoes suffer from a severe air pollution problem. Annual average coarse (diameter, $d_p > 2.1$ μm) particle concentrations measured outdoors at the Grottoes by our research group during a 1-yr period averaged 378 $\mu g\,m^{-3}$ (Salmon *et al.*, 1994). Peak 24-h average coarse particle concentrations of up to 1200 $\mu g\,m^{-3}$ were measured during April 1991. These airborne particles enter the caves and deposit onto the surfaces of the statues and carvings inside. Measurements show that horizontal surfaces become completely covered by a monolayer of dark-colored particles within about 0.13 yr at present (Christoforou *et al.*, 1994). Over the period 1986–1991, particle deposits as deep as 0.8 cm accumulated on surfaces inside the caves. One important source of particulate air pollution at the Grottoes is due to the coal dust and road dust generated by thousands of coal truck loads that travel daily along a highway that passes not more than 200 m to the south of the caves (Salmon *et al.*, 1995). Other sources of dust and smoke that affect the caves arise from soil dust generated by people working at or visiting the caves, vehicle traffic and human activity along the unpaved roads within the village of Yungang that is adjacent to the caves, burning of coal and wood in the village for heating and cooking, and seasonal wind/dust storms that blow from the Gobi desert.

Airborne particles enter the caves as air is exchanged between the outdoor atmosphere and the caves' interior. In order to understand the particle deposition problem, it is necessary to understand how much air is moving through the caves and the various factors that determine the air flow. The mechanism by which air enters and exits such cave temples is not well documented at present. Flow of air in and out of natural caves is sometimes due to changes in atmospheric pressure which leads to a phenomenon known as cave breathing (Wigley, 1967; Moore, 1978). Other previous investigations in mine shafts (Harris and Kingery, 1973) and also in natural caves (Wigley and Brown, 1976; Quindos *et al.*, 1987) have been undertaken that use natural convection to explain the air flows. Radon 222 concentration measurements have been made in order to define features of the natural circulation inside caves (Wilkening and Watkins, 1976). However, little is known about air exchange in man-made caves that are similar to those studied at Yungang. In particular, we seek enough information to be able to calculate how the air flow would respond to the reconstruction of the wooden temple buildings that once sheltered the entrances to the caves in antiquity and how the air flow would respond to the insertion of particle filtration material into the window panels of such temple building fronts.

EXPERIMENTAL METHODS

Two caves were chosen for analysis, Caves 6 and 9. As shown in Fig. 1, the entrances to Cave 9 through the rock cliff face are open directly to the outdoors. Cave 6, unlike Cave 9, retains its traditional wooden temple building that shelters the entrances through the cliff face. The surfaces of that building consist largely of narrow wooden door panels with a wooden lattice work backed by paper windows.

Between 12 April 1991 and 30 April 1991, experiments were conducted at Yungang to measure the airflow into and out of the caves using a battery of instruments. Thermoelectronic air velocity probes, hand-held mechanical air velocity meters and perfluorocarbon tracer (PFT) techniques were used to measure the air exchange rates. Measurements also were made that relate to the driving forces that cause the air flow. These include cave wall temperatures, indoor and outdoor air temperatures and outdoor wind speed and direction.

An omnidirectional air velocity probe (TSI model 1620) was placed near the center of the ground level entrance to Cave 9 (position 1 in Fig. 1a) and was used to record continuously the absolute value of the air velocity through that cave entrance. Periodic air velocity measurements were made at that entrance to Cave 9 using a hand-held mechanical air velocity meter (vaneometer, part no. 6610A4306, Whatman Labs, Hillsboro, OR) from which the speed and direction of the air flow into or out of the cave was noted as a function of time of day. The hand-held velocity meter also was used to measure air speed and direction through the ground floor entrance to the wooden temple building attached to Cave 6 (position 1 in Fig. 1b) with the wooden doors open, through the ground level opening in the rock wall between the antechamber and interior chamber of Cave 6 (position 2 in Fig. 1b) with the wooden temple front doors open and with the temple front doors closed, and through the upper level opening in the rock wall between the antechamber and the interior chamber of Cave 6 (position 3 in Fig. 1b) during two intensive periods of observation on 15–16 April and 24–25 April 1991. Air exchange rates also were measured both for the duration of the 20-day experiment and for each 4 h period during the 48 h intensive sampling experiment on 15–16 April using perfluorocarbon tracer (PFT) techniques (Dietz and Cote, 1982).

Cave wall temperatures and indoor air temperatures were measured by thermistor arrays that were placed at an elevation of 1.98 m above floor level inside both Caves 6 and 9. The cave wall temperature thermistors (part no. 44202, Yellow Springs Instrument Co., Yellow Springs, OH) were secured within shallow surface cracks in the cave walls using a thermal joint compound in order to ensure thermal contact with the wall. The air temperature thermistors were held in place 5.1 cm away from the surface of the cave walls. This placement was chosen in order to sample air temperatures within the fluid boundary layer along the cave walls. Outdoor air temperatures were recorded at the weather station operated by the Chinese government at the Yungang Grottoes.

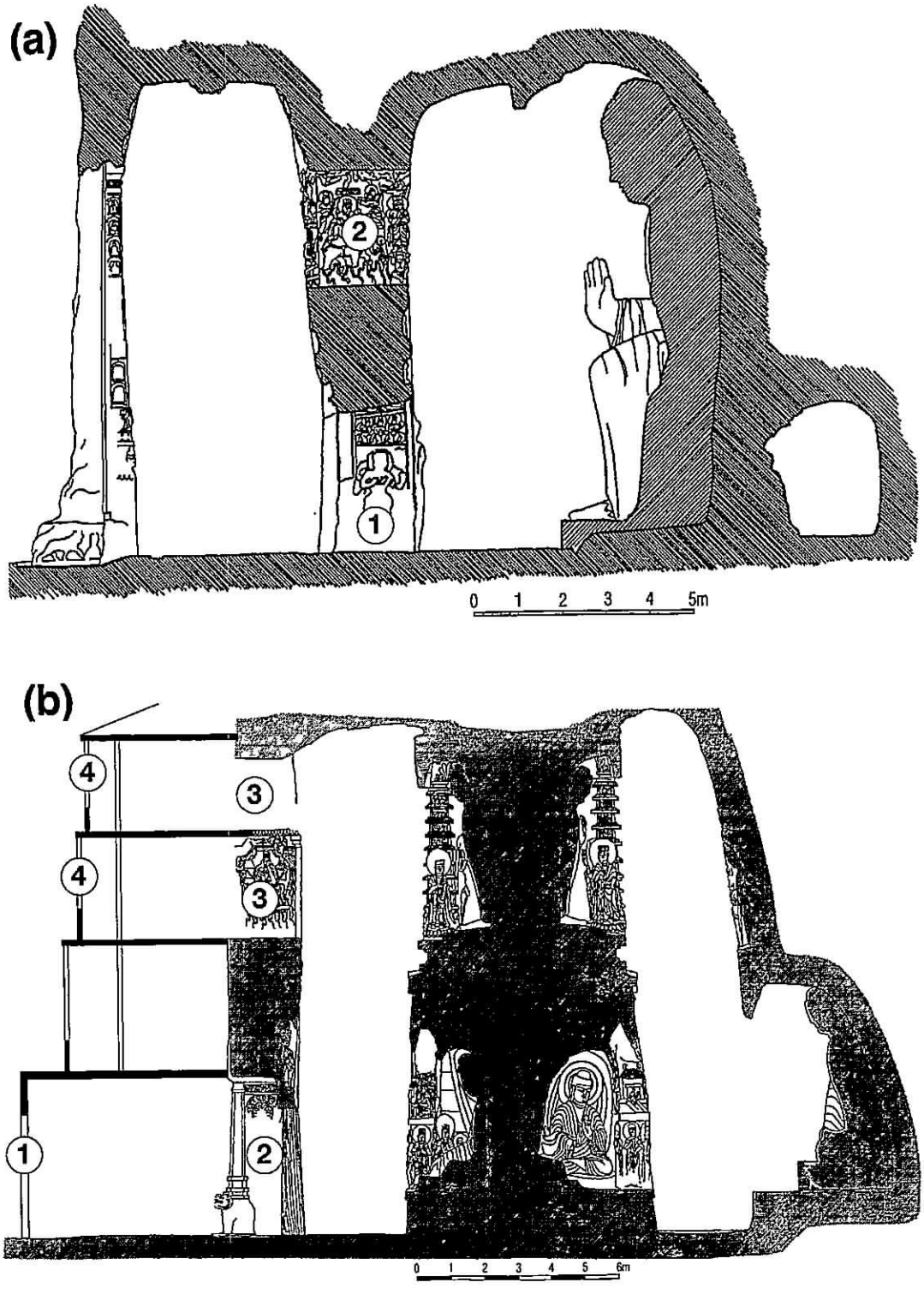

Fig. 1. Vertical cross-section of Cave 9 (top) and Cave 6 (bottom).

Natural convection boundary layer flows were expected along the interior vertical walls of the caves due to wall/air temperature differences. In order to confirm the magnitude of these flows, an omnidirectional velocity probe (TSI model 1620) was placed 1.65 m above ground level and 1 cm away from the cave walls. This probe was placed in Cave 9 during the first half of the experiment and in Cave 6 during the second half of the experiment.

Finally, wind speed and direction outdoors were recorded using an automated weather station (part no. 03001-5, Campbell Scientific Inc., Logan, UT). The purpose of these measurements was to determine whether or not pressure

differences induced by high-speed winds normal to or parallel to the face of the cliff containing the cave entrances were obviously influencing air motion through the caves.

With three exceptions, the above measurements were logged automatically every minute between 12 April 1991 and 30 April 1991 with the aid of a Campbell Scientific CR-10 measurement and control module. Temperature measurements inside Cave 6 and outdoors were recorded with the aid of a chart recorder, and the mechanical air velocity meter readings were recorded manually in laboratory notebooks.

RESULTS AND DISCUSSION

Figure 2 shows the air temperature outside the caves as well as the cave wall temperature and near-wall air temperature measurements made inside Cave 9 at 1.98 m above floor level. The indoor temperature data that were originally logged at 1 min intervals have been smoothed using a low-pass filter that removes fluctuations having a period shorter than 1 h. Figure 3 shows the temperature differences between the outdoor air and the near-wall air inside Cave 9 and also between the near-wall air inside Cave 9 and the cave walls.

Not surprisingly, the outdoor air is warmer during the day than it is at night. Peak hourly average outdoor air temperatures during the daytime over the days of the experiment were in the range 4.7–16.8°C, while the daily nighttime minimum hourly average temperatures outdoors were in the range −5.5 to 1.1°C. The temperature of the cave walls during April is typically less than the outdoor air temperature during the day, but is typically warmer than the outdoor air temperature during the night. For example, on 14 April 1991, hourly average outdoor air temperatures ranged from a low of −0.9°C at night to a high

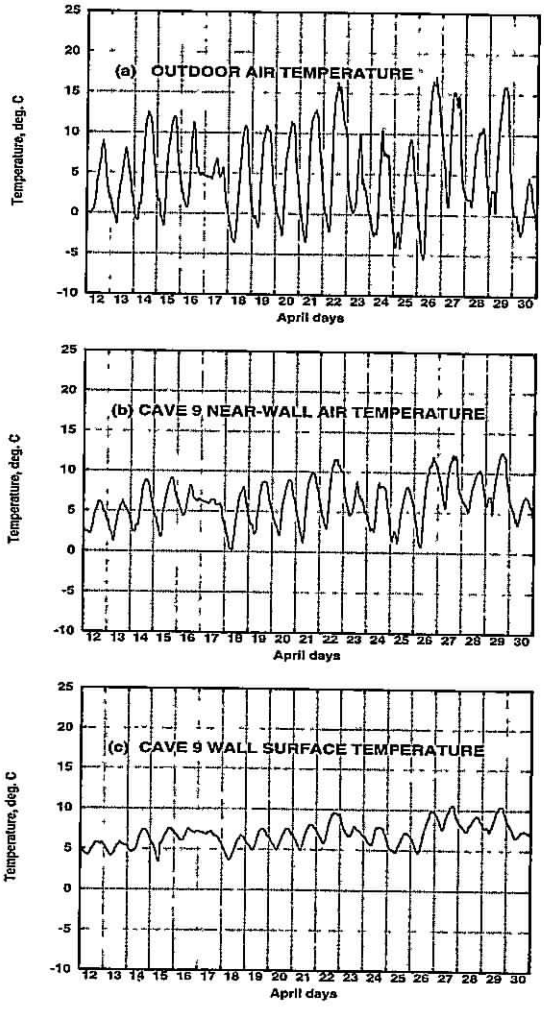

Fig. 2. Air temperatures and cave wall temperatures at Yungang, 12–30 April 1991: (a) shows the outdoor air temperature, (b) the air temperature measured 5.1 cm away from the vertical rock wall in Cave 9 and (c) the Cave 9 rock wall surface temperature.

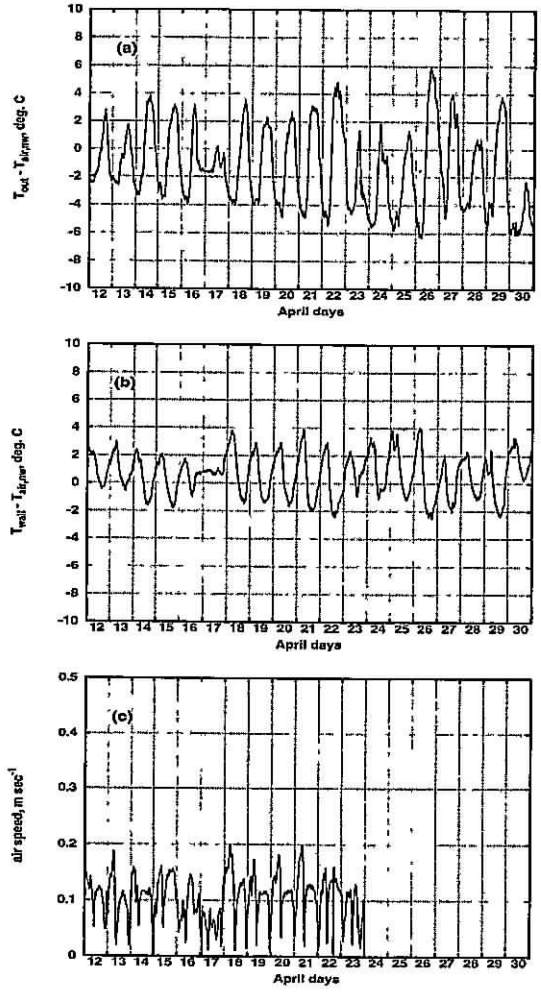

Fig. 3. Temperature differences and air speed along the cave walls at Yungang, April 1991: (a) temperature difference between the outdoor air, T_{out}, and the near-wall air inside Cave 9, $T_{air,nw}$, (b) wall surface temperature, T_{wall}, minus near-wall air temperature, $T_{air,nw}$, inside Cave 9, and (c) air speed in the boundary layer along the walls of Cave 9.

of 12.5°C in the afternoon, whereas during the same day hourly average cave wall surface temperatures inside Cave 9 ranged from a low of 4.6°C at night to a high of 7.1°C during the afternoon. Near-wall air temperatures inside the caves lie between those of the cave wall temperatures and the outdoor air temperatures. The near-wall air in the caves is warmer than the cave walls but cooler than the outdoor air during the day and the reverse is true at night. This means that the indoor air is denser than the outdoor air during the day and less dense than the outdoor air during the night. Wall–air temperature differences typically pass through zero around 1050 h in the morning and again around 2025 h at night. The outdoor and indoor air temperatures typically are periodic with a 24 h cycle, and this periodicity is reflected to a lesser extent in the daily cycling of the rock wall surface temperature. There is a long-term warming trend in the outdoor air over the course of the experiment that is reflected in a slow upward trend in the temperature of the cave wall surface, which suggests that seasonal cycling of the wall surface temperature occurs to some extent.

Wall temperature and near-wall air temperature cycles were observed inside Cave 6 that were similar to those seen inside Cave 9. Even though the average near-wall air temperature inside Cave 6 was almost the same as the average near-wall air temperature inside Cave 9 at the same height above ground level, the daytime near-wall air temperature peaks inside Cave 6 were lower than those inside Cave 9 by about 1.4°C, and the minimum nighttime near-wall air temperatures inside Cave 6 were warmer than the corresponding values inside Cave 9 by about 2.5°C. The situation was similar for the wall surface temperatures. The average of the daily peak 1 h average wall temperature values inside Cave 6 was 6.4°C (compared to 8.3°C for Cave 9), while the mean of the nighttime minimum 1 h average wall temperatures in Cave 6 was 5.1°C (compared to 4.2°C for Cave 9).

Figure 3c shows that the air speed along the wall in Cave 9 follows a natural convection pattern. That air flow is periodic, typically with two high flow events per day. One of these high flow events typically occurs between midnight and mid-morning each day and logically corresponds to flow up the wall at a time when the walls are warmer than the air in the caves. The second high flow event occurs during the afternoon and early evening when the cave walls are cooler than the air in the caves and logically corresponds to flow down the cool cave walls. Typically, when the wall-air temperature difference shown in Fig. 3b is near zero, so is the air velocity along the wall, and when the absolute value of the temperature difference is greatest, so is the air velocity near the walls.

The air velocity at the center of the ground level entrance of Cave 9 (position 1 in Fig. 1a) as recorded by the omnidirectional velocity probe is shown in Fig. 4a. Figure 4b shows the same data set after the data have been smoothed and with the air flow direction stated based on the records from the hand-held mechanical velocity meter. In Fig. 4b, a positive air velocity denotes air flow from outdoors into Cave 9 through the ground level entrance (position 1 in Fig. 1a) accompanied by flow out of the third-floor level exit (position 2 in Fig. 1a) from the cave while negative velocity indicates flow in the reverse directions. The velocity is periodic during the course of the day. It goes to zero twice, first sometime typically around 0930 h in the morning and then again around 2100 h at night.

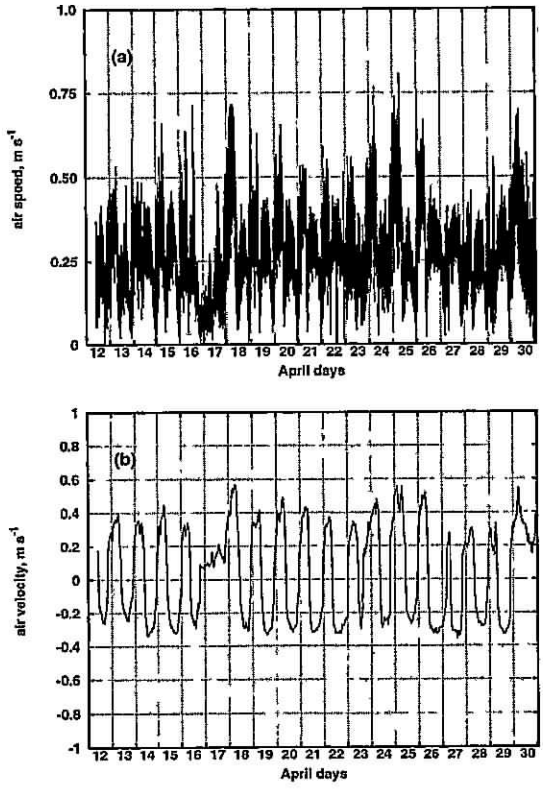

Fig. 4. Air flows at the entrance to Cave 9 at Yungang, April 1991: (a) air speed measured in the ground level entrance to Cave 9 (position 1 in Fig. 1a), and (b) smoothed air velocity data from (a) above with the direction of the air flow assigned based on periodic mechanical air velocity meter readings. Positive velocity indicates flow of air into the cave at the ground level entrance.

Air flow through the entrance of Cave 9 can be explained with the aid of Fig. 3. Late at night and in the early morning when the cave wall is warmer than both the outdoor air and the air in the cave, air rises along the walls; air that is warmer than that outdoors accumulates and exits the cave from the opening that exists in the rock wall at the third floor level, while cooler outdoor air enters the cave through the main ground level entrance to replace the warm air leaving at the upper level exit. As the wall/air temperature difference and the indoor/outdoor air temperature difference decreases, so does the magnitude of the air velocity in the entrance to the cave. As the outdoor air is warmed during the day, eventually the temperature

of the air entering Cave 9 becomes greater than the cave wall surface temperature. Around mid-morning, the flow of air through the cave entrance reverses direction and then begins to increase. Warm outdoor air is drawn into the cave through the opening at the third-floor level and then is cooled by contact with the colder cave walls; cold air accumulates and then flows out through the ground floor main entrance. This outflow at ground level continues until about 2100 h at night, at which time the outdoor air temperature and the air temperature inside Cave 9 again become nearly equal to the wall temperature, in which case the air exchange is reduced to nearly zero. Next, air starts flowing into the cave through the ground level main entrance as the interior air temperature falls below that of the cave wall temperature, and the cycle continues. The mean air speed at the center of the entrance of Cave 9 is $0.274\,m\,s^{-1}$ averaged over the April 1991 experiments.

To compute the air volume entering or leaving Cave 9, it is necessary to know the air velocity distribution across the entrance through the rock wall where the omnidirectional velocity probe was placed. The hand-held mechanical velocity meter was used to make measurements each hour at a matrix of nine points across the face of that entrance over three 24 h periods. The mechanical velocity meter data were then averaged to determine the volume-weighted average air velocity entering Cave 9. Regression of air velocity at the center of the door on the volume-weighted average air velocity through the door results in a slope of 1.06 ± 0.05, an intercept of $-0.07 \pm 0.04\,m\,s^{-1}$ and a correlation coefficient of 0.91. Therefore, the air flow through the Cave 9 entrance is approximately a plug flow and the velocity measurement taken at the center of the entrance is sufficient to describe the air flow in or out of the caves.

Using the smoothed omnidirectional velocity probe measurements in the entrance of Cave 9 and the dimensions of the entrance, the average air volume flowing through Cave 9 was calculated to be $7300\,m^3\,h^{-1}$ or $121\,m^3\,min^{-1}$ averaged over the period 12–30 April 1991. At that flow rate, one complete air exchange is achieved within Cave 9 in only 4.3 min on average. The daytime peak 1 h mean volumetric air flow rate out of the lower entrance of Cave 9 during April 1991 averaged $288\,m^3\,min^{-1}$ (33 air changes per hour), while the nighttime 1 h peak volumetric flow rate in the reverse direction averaged $175\,m^3\,min^{-1}$ (20 air changes per hour).

Air flow rates through the caves also were measured using the perfluorocarbon tracer technique. Averaged over the entire duration of the experiment, the volume of air flowing through Caves 6 and 9 was measured to be $8620 \pm 1480\,m^3\,h^{-1}$ and $8190 \pm 1240\,m^3\,h^{-1}$, respectively. The result obtained for Cave 9 from the tracer experiment is clearly in reasonable agreement with the result obtained from the omnidirectional velocity probe at the entrance to Cave 9. Since Cave 6 is approximately four times larger in volume than Cave 9, the rough equality of long-term average volumetric air flow rates means that the time to achieve one complete air exchange inside Cave 6 is approximately 4 times longer than Cave 9. This factor of four difference in air exchange times occurred under the condition where several of the door panels present in the upper stories of the wooden temple structure in front of Cave 6 typically were in their open position, providing less resistance to air exchange than would be the case if those doors were tightly closed (we did not seek to alter the settings of those doors; Cave 6 was examined exactly as it was operated by the Grottoes staff).

Figure 5a shows the outdoor wind speed component parallel to the cliff face that contains the cave entrances, with a positive wind speed taken when wind blows from west to east across the cave entrances. Figure 5b shows the wind speed component perpendicular to the cave entrances, with a positive component designating flow from south to north toward the front of the cliff face. Earlier, it was seen that air flow into and out of Cave 9 closely tracked changes in the air temperature data. When the outdoor wind speed data of Figs 5a and b are compared to the bulk

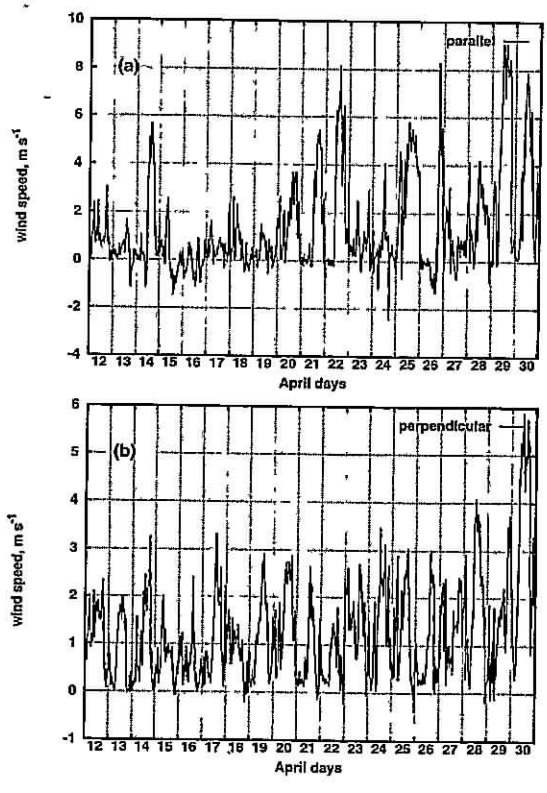

Fig. 5. Outdoor wind speed at Yungang, April 1991: (a) wind speed component parallel to the front of the cliff into which the caves are carved. Positive values indicate flow from the west to the east in front of the entrance to Cave 9, while negative numbers indicate flow from east to west. (b) Wind speed component perpendicular to the cliff face. Positive values indicate flow from south to north toward the entrances to Cave 9.

air exchange through Cave 9 that is shown in Fig. 4b, it is seen that there is little obvious effect of outdoor wind speed changes on air exchange rate changes: high wind speed days like 28–30 April show air exchange rates comparable to most other days examined, as do low wind speed days like 18 April. It is concluded that air exchange through these caves is driven largely by a thermally induced natural convection flow with outdoor wind speed changes contributing at most a secondary effect.

THEORETICAL MODEL

Cave 9

A theoretical model is now presented that accounts for the bulk air exchange between outdoors and the inside of Cave 9 as seen in the filtered air velocity data. Consider first the case where warm air flows into Cave 9 through the upper level entrance shown at position 2 in Fig. 1a. The air is cooled by contact with the cave walls; cool air accumulates within the core of the cave and next exits through the ground level opening in the cave wall at position 1 in Fig. 1a. The following three equations are used:

$$\frac{\mathrm{d}}{\mathrm{d}t}(\rho_a V) = \rho_o U_2 A_2 - \rho_a U_1 A_1 \tag{1}$$

$$\frac{\mathrm{d}}{\mathrm{d}t}(\rho_a V c_v T_a) = \rho_o U_2 A_2 c_p T_o - \rho_a U_1 A_1 c_p T_a - \sum_{i=1}^{3} h_i S_i (T_a - T_w) \tag{2}$$

$$\tfrac{1}{2}\rho_o U_2^2 C_L + \tfrac{1}{2}\rho_a U_1^2 C_L = gH(\rho_a - \rho_o) \tag{3}$$

where ρ_a is the bulk density of the air mass inside the cave, ρ_o is the density of air outside the cave, T_a is the absolute temperature of the air inside the central core of the cave, T_o is the absolute temperature of the air outside the cave, T_w is the absolute temperature of the cave rock walls, V is the volume of the cave, H is the elevation difference between the air entering the cave and the air leaving the cave, A_1 is the cross-sectional area of the cave entrance at ground level, A_2 is the cross-sectional area of the opening in the cave rock wall at the third floor level, c_p is the specific heat of air at constant pressure (1006 $\mathrm{J\,kg^{-1}\,°C^{-1}}$), c_v is the specific heat of air at constant volume (719 $\mathrm{J\,kg^{-1}\,°C^{-1}}$), g is the acceleration due to gravity (9.81 $\mathrm{m\,s^{-2}}$), C_L is the loss coefficient for air flow through the openings in the rock walls of the cave (taken to be 1.5 as for induction of air into a building from outdoors (Jennings and Lewis, 1965), and for flow through a square edged orifice (Sabersky *et al.*, 1989)), and h_i is the heat transfer coefficient for natural convection boundary layer flow over the ith cave surface. The heat transfer surface areas of the cave walls, floor, and ceiling are given by S_1, S_2, and S_3, respectively, and the heat transfer coefficients at the walls, floors, and ceilings are h_1, h_2, and h_3, respectively. U_2 is the air velocity entering the cave at the opening through the rock wall at the third-floor level and U_1 is the air velocity exiting the cave at the ground floor level, with both velocities taken as positive in the direction of flow. The numerical values for geometric parameters H, A_1, A_2, V, S_1, S_2 and S_3 for Cave 9 are given in Table 1.

Equations (1), (2), and (3) above are essentially the continuity equation, an equation stating that the change in internal energy of the air inside the cave over time depends on energy convected in and heat

Table 1. Geometric parameters of Caves 6 and 9

Parameter	Description	Cave 6	Cave 9
Z	Physical height of the cave	15 m	10.35 m
H	Elevation difference between entering and exiting critical fluid streamline	9.25 m	2.39 m
V	Volume of cave	2222 m^3	528 m^3
S_1	Nominal wall surface area based on major outline of walls[a]	1370 m^2	346.6 m^2
S_2	Nominal ceiling surface area of cave	163 m^2	43.7 m^2
S_3	Floor surface area of cave	179 m^2	43.7 m^2
A_1	Cross-sectional area of entrance through rock wall at ground level, Cave 9		7.4 m^2
A_2	Cross-sectional area of opening in rock wall at third and fourth floor level, Cave 9		5.6 m^2
A_{1a}	Cross-sectional area of openings in building shell downstairs, Cave 6, front door open	4.8 m^2	–
A_{1b}	Cross-sectional area of openings in building shell downstairs, Cave 6, front door closed	0.46 m^2	–
A_2	Cross-sectional area of entrance through rock walls at ground level, Cave 6	11.8 m^2	–
A_3	Cross-sectional area of opening in rock wall at third and fourth floor level, Cave 6	21.1 m^2	–
A_4	Cross-sectional area of openings in building shell upstairs, Cave 6	4.2 m^2	–

[a] The walls are covered with Buddhist sculptures in high relief; we estimate the actual surface area of the carvings to be about twice the nominal area defined by the major outline of the cave walls.

transfer at the cave walls less energy convected out, and an equation that balances the pressure drops in the air path against the density differences between the indoor vs outdoor air acting on the height of the air column between the entering and exiting air paths, respectively. In writing the set of equations, the following approximations were made: (a) air inside the cave is well mixed, (b) flow through the openings between outdoors and the cave interior is plug flow, (c) flow starts due to a pressure difference due to air density differences between the interior of the cave and the outdoors, and (d) there is a natural convection boundary layer flow along the cave walls that is due to wall/air temperature differences that leads to heat transfer between the cave walls and the air in the caves.

In the system of equations (1)–(3), the velocities at the entrances (U_1 and U_2), the temperature and density of the air inside the core of the cave, T_a and ρ_a, respectively, are the unknowns. To solve the system, the following approximations are made: (a) $\rho_a \approx \rho_o \approx \rho$ except that $(\rho_a - \rho_o)/\rho_o \neq 0$, and also $(\rho_a - \rho_o)/\rho_o \approx (T_o - T_a)/T_o$. The equations then can be written

$$U_1 A_1 = U_2 A_2 \tag{4}$$

$$\rho c_v V \frac{d}{dt}(T_a) = \rho c_p (U_2 A_2 T_o - U_1 A_1 T_a) - \sum_{i=1}^{3} h_i S_i (T_a - T_w) \tag{5}$$

$$U_1^2 + U_2^2 = \frac{2gH|T_o - T_a|}{C_L \quad T_o}. \tag{6}$$

Equations (4), (5), and (6) may be solved for U_1, U_2, and T_a.

The solution for the velocity at the cave entrance, U_1 is

$$U_1 = \left(\frac{2gHA_2^2 |T_o - T_a|}{C_L (A_1^2 + A_2^2) T_o} \right)^{0.5}. \tag{7}$$

The time rate of change of the air temperature in the core of the cave becomes

$$\frac{d}{dt}(T_a) = \frac{1}{V \rho c_v} \left(\sum_{i=1}^{3} h_i S_i (T_w - T_a) + A_1 A_2 \rho c_p \left(\frac{2gH|T_o - T_a|}{C_L (A_1^2 + A_2^2) T_o} \right)^{0.5} (T_o - T_a) \right). \tag{8}$$

Given a continuous series of data on cave wall temperatures and outdoor air temperature and density, plus an initial value for the indoor air temperature in the core of the cave, equation (8) may be solved to predict air temperatures inside the core of the cave over time provided that the heat transfer coefficients can be estimated. Equation (7) may then be used to calculate the air velocity at the entrance of the cave from the outdoor temperatures and the predicted cave air temperature. An analogous set of equations can be written to describe the condition where cold air enters the ground floor entrance to the cave and is warmed by contact with the warmer cave walls. A model for predicting air exchange through the cave based on the difference between the outdoor air temperature and the cave wall temperature thus results.

The heat transfer coefficient at the surface of the cave walls first must be specified. A relationship for the Nusselt number for natural convection flow over a vertical flat plate is provided by Churchill and Chu (1973):

$$\overline{Nu}_Z = \left(0.825 + \frac{0.387 Ra_Z^{1/6}}{[1 + (0.492/Pr)^{9/16}]^{8/27}} \right)^2 \tag{9}$$

$$\overline{Nu}_Z = \frac{Z h_1}{k} \tag{10}$$

$$Ra_Z = Pr \frac{g(T_w - T_a) Z^3}{T_a \nu^2} \tag{11}$$

where $\overline{Nu}_Z$ is the Nusselt number averaged over the length of the plate (in this case the height, Z, of the cave walls), Ra_Z is the Rayleigh number based on the height of the cave walls, Pr is the Prandtl number for air, k is the thermal conductivity of air, and ν is the kinematic viscosity of air. Heat transfer rates from the cave floor and ceiling vary depending on whether the heating or cooling there favors atmospheric stability or instability. A heated upward facing surface (the floor) or a cooled downward facing surface (the ceiling) creates instability. This situation will be represented as if the floors and ceilings were independent heated or cooled flat plates, for which Incropera and DeWitt (1984) provide the heat transfer estimates:

$$\overline{Nu}_L = 0.54 Ra_L^{1/4} \quad 10^4 < Ra_L < 10^7 \tag{12}$$

$$\overline{Nu}_L = 0.15 Ra_L^{1/3} \quad 10^7 < Ra_L < 10^{11}. \tag{13}$$

Both the Ra_L and Nu_L are based on the characteristic length L that is computed as the area of the surface divided by the perimeter of the surface. Equations (12) and (13) will be used to estimate the heat transfer coefficient, h_2, for the cave floor when $T_w > T_a$ and the heat transfer coefficient, h_3, for the cave ceiling when $T_a > T_w$, where the floor and ceiling temperatures are taken to be at the measured temperature of the cave rock walls. When the floor is colder than the air in the cave or when the ceiling is warmer than the cave air the expression

$$\overline{Nu}_L = 0.27 Ra_L^{1/4} \tag{14}$$

is used to estimate h_2 for the cave floor when $T_a > T_w$ and h_3 for the cave ceiling when $T_w > T_a$ over the range $10^5 < Ra_L < 10^{10}$ (Incropera and DeWitt, 1984).

While natural convection flow over a flat vertical plate is analogous to the natural convection flow observed along the walls of the caves at Yungang, the

analogy cannot be exact. This is because the cave walls are not actually flat. Instead, they are covered with Buddhist carvings in high relief that both add to the actual surface area and that may interrupt the boundary layer air flow. Both of these factors would be expected to enhance heat transfer beyond that seen over a flat plate having the nominal height of the cave walls. For that reason, a semi-empirical adjustment to the model is used. Having examined detailed photographs of the cave walls, we estimate that the actual surface area of the carvings is about 2 times larger than the nominal surface area of the major outline of the cave walls. Therefore, the value of the product $h_i S_i$ appearing in equation (8) applied during the calculations for Cave 9 is taken to be twice as large as would be the case for a vertical flat plate having the nominal surface area of the major outline of the cave walls.

Equation (8) may be solved for T_a given T_o and T_w. The differential equation (8) is integrated for 60 s given fixed values for T_o and T_w. At the end of 60 s the values of T_o and T_w are updated from the experimental data base, the value of T_a predicted at the end of the previous 60 s is used as the initial value for the next calculation cycle and thus the solution is continued. From the resultant time series of predicted values for T_a, the air velocity through the ground level entrance to Cave 9 as a function of time is obtained from equation (7), with the direction of flow specified according to the sign of the temperature difference $(T_o - T_a)$. Figure 6a shows the near-wall air temperature, $T_{air,nw}$, predicted by the model at a distance 5.1 cm from the wall and 1.98 m from the floor inside Cave 9, together with the measured indoor near-wall air temperature at that location compared to the outdoor air temperatures and cave wall temperatures supplied to the model. The predicted value of $T_{air,nw}$ is obtained from values of T_a predicted by the model by noting that the shape of the thermal boundary layer for turbulent natural convection flow along a vertical flat plate (see Eckert and Jackson, 1951) is approximately given by

$$T_{air,nw} = T_a + (T_w - T_a)\left(1 - \left(\frac{y}{\delta}\right)^{1/7}\right) \quad (15)$$

$$\delta = 0.565x(Gr)^{-1/10}(Pr)^{-8/15}[1 + 0.494(Pr)^{2/3}]^{1/10} \quad (16)$$

where δ is the thickness of the boundary layer, y is the distance from the cave wall, and x is the distance from the starting point of the boundary layer flow. Gr is the Grashof number

$$Gr = \frac{g\beta(T_w - T_a)x^3}{\nu^2} \quad (17)$$

and β is the expansion coefficient of the air which is estimated to equal T_a^{-1} with T_a stated in degrees Kelvin. The distance x is taken to be the distance from the cave ceiling to the thermistor that measures

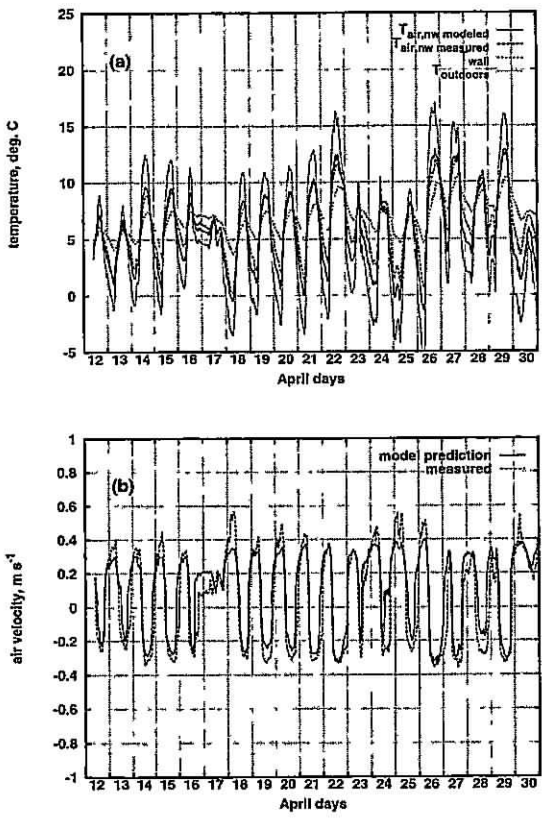

Fig. 6. Results of the cave air exchange model at Cave 9: (a) measurements and model predictions of near-wall air temperatures inside Cave 9, compared to measured outdoor air temperatures and measured cave wall temperatures supplied to the model, (b) measurements and model predictions of air velocity through the ground level entrance to Cave 9. A positive velocity value indicates flow into the ground level entrance to Cave 9, while a negative velocity value indicates flow out of the ground level entrance at position 1 in Fig. 1a.

$T_{air,nw}$ for flow down the wall and to be the distance from the cave floor to that thermistor for flow up the wall. The mean of the absolute value of the paired 1 min average temperature differences between $T_{air,nw}$ predicted vs the smoothed $T_{air,nw}$ observations is 0.86°C.

Figure 6b shows a comparison of measured and predicted air velocities at the ground level entrance of Cave 9. In general, good agreement is obtained between the model predictions and the observations of the air flows through Cave 9. Peak flows are underpredicted to some degree. If either the heat transfer coefficient or the interior wall surface area were increased, almost exact agreement between predictions and observations could be achieved.

Cave 6

Cave 6 still retains a wooden temple building in front of the cave entrances. A model for the air flow through Cave 6 must therefore be more elaborate. The building shell is represented as a series of pressure loss terms that are added to the LHS of equation (3).

Specifically, a pressure drop term is added to represent flow of air through the cracks around the wooden door panels that cover the temple structure at the third-floor and fourth-floor levels at positions 4 in Fig. 1b. Another pressure drop term results from the flow of air through the ground-floor level of the wooden building shell at position 1 in Fig. 1b. The latter term varies depending on the time of the day: during the daytime the front doors are kept opened, while at night the doors are closed and air is forced to exit through the various cracks and openings around the doors and in the building shell. The small additional pressure drops that occur due to the flow of air across the downstairs anteroom, and across the upstairs anterooms of Cave 6 were computed and found to be negligible.

There are no reliable data for some of the geometric parameters for Cave 6. One such parameter is the area of the cracks and openings in the building shell on the third floor and fourth floor levels. In order to obtain a better estimate of that number, a modified version of equation (6) is written for Cave 6 for the case where the front doors at ground level are open (i.e. during daytime):

$$C_L U_4^2 + C_L U_3^2 + C_L U_2^2 + C_L U_{1a}^2 = \frac{2gH|T_o - T_a|}{T_o} \tag{18}$$

where the various subscripts are coordinated with the labels in Fig. 1b, as follows: position 4 refers to the cracks and openings in the upstairs building shell, position 3 to the opening in the rock wall of the cave upstairs, and position 2 to the opening in the rock wall of the cave downstairs, while the subscript 1a signifies the condition at the downstairs front entrance doors to the wooden temple structure with these doors open. The cracks and openings in the upstairs building shell range from open door panels to rectangular slots between panels. Since all openings at positions 1–4 are rectangular, the same loss coefficient, C_L, as was cited previously for use with the rectangular entrance at Cave 9 will be applied to each flow restriction term. The many openings in the building shell at the third- and fourth-floor level at Cave 6 act in parallel and therefore experience the same pressure drop. If the loss coefficient is roughly the same for each of these openings, then the velocities through the openings in the building shell at the third and fourth floor levels will be similar, and one term will suffice in equation (18) to describe the product of the square of that velocity times the loss coefficient.

Using the continuity equation, all velocities in equation (18) can be expressed in terms of the velocity at the downstairs opening in the rock wall of the cave, U_2, and the dimensions of the various openings in the air path where those velocities prevail. The velocity through the cracks upstairs, U_4, thus can be expressed as a function of U_2 and the as yet unknown area of the cracks upstairs, A_4. Spot measurements of the air velocity through the downstairs opening in the rock wall of Cave 6 (at position 2 in Fig. 1b) were made periodically during these experiments using the hand-held mechanical velocity meter. Using measured values of U_2, T_a, and T_o taken at various hours during our experiments along with measured values of the size of the openings at positions 1a, 2, and 3 in Fig. 1b, as shown in Table 1, equation (18) is used to estimate the area of the cracks and openings upstairs. Doing so gives a cross-sectional area of the cracks and openings upstairs $A_4 = 4.09\ \text{m}^2 \pm 2.09$, which is larger than the value of $A_4 = 1.75\ \text{m}^2$ that we estimated by visual inspection for cracks around the upper-floor door panels while at Yungang. The reason for the discrepancy is simple. Our photographs show that some of the door panels at the third-floor level ($A \approx 1.67\ \text{m}^2$ for each door panel) or one of the side doors ($A \approx 2.65\ \text{m}^2$) were frequently left open by persons passing through the temple structure, thus increasing the effective cross-sectional area of the openings at the third-floor level beyond the value that would be due to cracks between door panels.

The numerical model for air flow through Cave 9 was modified to correspond to the geometric parameters given for Cave 6 in Table 1 and to represent the additional pressure drops present at Cave 6. Then the time series of outdoor temperatures and cave wall temperatures was supplied to the model in order to calculate the air temperature expected inside Cave 6 and the air flows through Cave 6. Again, the product of the heat transfer coefficient times the vertical wall surface area was taken to be twice as large as that estimated from examining the major outline of the cave walls, just as was done for Cave 9. From 0700 h each morning until 2000 h each evening, when Cave 6 is open to visitors or staff, flows were calculated with the downstairs entry doors open, while from 2000 h each evening until 0700 h in the morning, air flows were calculated with the downstairs doors closed.

Figure 7a shows the near-wall air temperature predictions inside Cave 6 together with the measured indoor near-wall air temperature in Cave 6 compared to outdoor air temperatures and cave wall temperatures supplied to the model. The same general conclusions hold true for Cave 6 as were observed for Cave 9. Reasonable agreement is evident between the measured and predicted near-wall air temperature values inside Cave 6. The mean of the absolute differences between $T_{\text{air,nw}}$ predicted and observed is 0.59°C, in spite of the fact that the strip chart recorder that recorded temperature values for the cave wall and $T_{\text{wall}} - T_{\text{air,nw}}$ can be read no more closely than $\pm$ 0.5°C. Figure 7b shows the predicted air velocity at the ground level passage through the rock wall between the antechamber and the interior chamber of Cave 6 at position 2 in Fig. 1b, together with velocity measurements taken during 15–16 April 1991 using the mechanical air velocity meter at the same location. Velocities calculated at that location from the results of the short-term perfluorocarbon tracer tube (PFT)

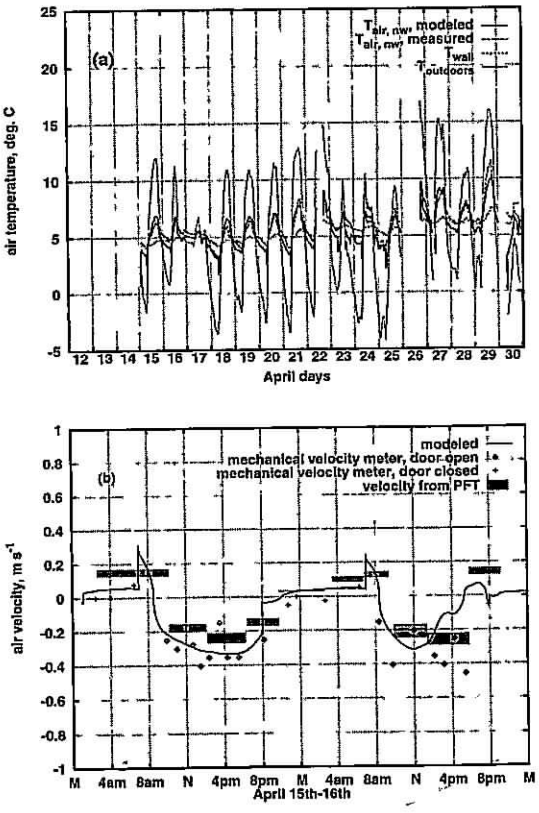

Fig. 7. Results of the cave air exchange model at Cave 6: (a) measurements and model predictions of near-wall air temperature inside Cave 6 compared to measured outdoor air temperatures and measured cave wall temperatures supplied to the model, (b) measurements and model predictions of air velocity in the ground level passage through the rock wall of Cave 6 at position 2 shown in Fig. 1b, on 15–16 April 1991. A positive velocity value indicates flow into the ground level entrance to Cave 6, while a negative velocity value indicates flow out of the ground level entrance at position 2 in Fig. 1b. The main front doors to the temple are modeled as being open during the day and closed at night.

experiment also are shown. There is general agreement between the model predictions and the air flow measurements, with the model predictions falling between the results of the PFT and mechanical velocity meter readings. The model calculations find that the air flow through Cave 6 averaged 5940 $m^3 h^{-1}$ or 99 $m^3 min^{-1}$ over the 15–16 April 1991 period. This corresponds to one complete air exchange at Cave 6 every 22 min on average during the 15–16 April period modeled in Fig. 7b, which is a lower air exchange rate than the long-term average air exchange rate observed for the whole month as described earlier.

CONCLUSIONS

A computer-based model has been developed that can predict air flows into and out of the Buddhist cave temples at Yungang. These air exchange rates govern the severe particle deposition problem within the caves by altering the number of particles entering the caves over time (Nazaroff and Cass, 1991). Air exchange rates also affect the rate at which water vapor (arising from water seepage through the cave rock surface, which damages the sculptures) can be exhausted from the caves. An ability to compute air exchange rates and how they respond to changes in meteorological conditions and to changes in the way that the structures in front of some caves are operated thus is of major importance to future efforts to conserve the Grottoes. The model takes as input cave dimensions, outdoor air temperatures, and indoor cave wall temperatures and predicts indoor air temperatures and air flows into and out of the caves according to the cooling of the air within the caves that is predicted to occur due to natural convection heat transfer along the cave walls. The model has the capability of accepting as further input resistances to air flow that would arise if filter material were installed in the surface of an existing or reconstructed wooden shelter in front of a cave in order to remove particulate matter from the air. Data gathered at Yungang during an extensive monitoring program in April 1991 were used for verification of the model. The results show good agreement between observed vs predicted air flows and air temperatures, both in the case of Cave 9 (a cave without extra flow resistances), and Cave 6 (a cave that has extra flow resistances in the form of the wooden temple structure that stands over the entrances to that cave).

Acknowledgements—This work was supported by a research agreement from the Getty Conservation Institute (GCI). The cooperation and assistance of the staff of the Yungang Grottoes and the State Bureau of Cultural Relics is gratefully acknowledged, including Huang Kezhong, Zhu Changling, Sheng Weiwei, Li Xiu Qing, Li Hua Yuan, Xie Ting Fan, Yuan Jin Hu, Huang Ji Zhong, Zhi Xia Bing, Bo Guo Liang of the Shanxi Institute of Geological Sciences, and Zhong Ying Ying from Taiyuan University. Assistance critical to this work was provided by the GCI and their consultants, and we especially thank Neville Agnew, Po-Ming Lin, Shin Maekawa, and Roland Tseng for their help.

REFERENCES

Christoforou C. S., Salmon L. G. and Cass G. R. (1994) Deposition of atmospheric particles within the Buddhist cave temples at Yungang, China. *Atmospheric Environment* **28**, 2081–2091.

Churchill S. W. and Chu H. H. S. (1975) Correlating equations for laminar and turbulent free convection from a vertical plate. *Int. J. Heat Mass Transfer* **18**, 1323–1329.

Cox L. B. (1957) *The Buddhist Cave-Temples of Yün-Kang & Lung-Men.* The Australian National University, Canberra.

Dietz R. N. and Cote E. A. (1982) Air infiltration measurements in a home using a convenient perfluorocarbon tracer technique. *Envir. Int.* **8**, 419–433.

Eckert E. R. G. and Jackson T. W. (1951) Analysis of turbulent free-convection boundary layer on flat plate. NACA Report No. 1015.

Harris E. J. and Kingery D. S. (1973) Ventilation. In *SME Mining Engineers Handbook* (edited by Given I. A.). Port City Press, Baltimore, Maryland.

Incropera F. P. and DeWitt D. P. (1985) *Fundamentals of Heat and Mass Transfer*. Wiley, New York.

Knauer E. R. (1983) The fifth century A.D. Buddhist cave temples at Yün-Kang, North China. *Expedition* **25** (summer), 27–47.

Jennings B. H. and Lewis S. R. (1965) *Air Conditioning and Refrigeration*, 4th Edn, Chap. 12. International Textbook Company, Scranton, Pennsylvania.

Nazaroff W. W. and Cass G. R. (1991) Protecting museum collections from soiling due to deposition of airborne particles. *Atmospheric Environment* **25A**, 841–852.

Moore G. W. (1978) *Speleology: The Study of Caves*. Zephyrus Press, Teaneck, New Jersey.

Quindos L. S., Bonet A., Diaz-Caneja N., Fernandez L. P., Gutierrez I., Solana R. J., Soto J. and Villar E. (1987) Study of the environmental variables affecting the natural preservation of the Altamira cave paintings located at Santillana Del Mar, Spain. *Atmospheric Environment* **21**, 551–560.

Sabersky R. H., Acosta A. J. and Hauptmann E. G. (1989) *Fluid Flow, A First Course in Fluid Mechanics*, 3rd Edn, Chap. 3. Macmillan, New York.

Salmon L. G., Christoforou C. S. and Cass G. R. (1994) Airborne pollutants in the Buddhist cave temples at the Yungang Grottoes, China. *Envir. Sci. Technol.* **28**, 805–811.

Salmon L. G., Christoforou C. S., Gerk T. J., Cass G. R., Casuccio G. S., Cooke G., Leger M. and Olmez I. (1995) Source contributions to airborne particle deposition at the Yungang Grottoes China. *Sci. Tot. Envir.* **167**, 33–47.

Sickman L. and Soper A. (1968) *The Art and Architecture of China*. Yale University Press, Pelican History of Art, New Haven and London.

Wigley T. M. L. (1967) Non-steady flow through a porous medium and cave breathing. *J. geophys. Res.* **72**, 3199–3205.

Wigley T. M. L. and Brown M. C. (1976) The physics of caves. In *The Science of Speleology* (edited by Ford T. D. and Cullingford C. H. D.). Academic Press, New York.

Wilkening H. M. and Watkins D. E. (1976) Air exchange and ^{222}Rn concentrations in the Carlsbad caverns. *Health Phys.* **31**, 139–145.